Toxicology in Vitro 30 (2015) 79–94

Contents lists available at ScienceDirect

Toxicology in Vitro

journal homepage: www.elsevier.com/locate/toxinvit

Determination of liver specific toxicities in rat hepatocytes by high content imaging during 2-week multiple treatment

Davide Germano, Marianne Uteng, Francois Pognan, Salah-Dine Chibout, Armin Wolf*

Discovery and Investigative Safety, Preclinical Safety, Novartis Institutes for Biomedical Research, CH-4057 Basel, Switzerland

ARTICLE INFO

Article history:
Received 27 January 2014
Accepted 19 May 2014
Available online 14 June 2014

Keywords:
High content imaging
Rat hepatocytes
Hepatotoxicity
In vitro model
Long-term culture
Safety profiling

ABSTRACT

DILI is a major safety issue during drug development and one of the leading causes for market withdrawal. Despite many efforts made in the past, the prediction of DILI using *in vitro* models remains very unreliable. In the present study, the well-established hepatocyte Collagen I-Matrigel™ sandwich culture was used, mimicking chronic drug treatment after multiple incubations for 14 days. Ten drugs associated with different types of specific preclinical and clinical liver injury were evaluated at non-cytotoxic concentrations. Mrp2-mediated transport, intracellular accumulation of neutral lipids and phospholipids were selected as functional endpoints by using Cellomics™ Arrayscan® technology and assessed at five timepoints (day 1, 3, 7, 10, 14). Liver specific functional impairments after drug treatment were enhanced over time and could be monitored by HCI already after few days and before cytotoxicity. Phospholipidosis-inducing drugs Chlorpromazine and Amiodarone displayed the same response as *in vivo*. Cyclosporin A, Chlorpromazine, and Troglitazone inhibited Mrp2-mediated biliary transport, correlating with *in vivo* findings. Steatosis remained difficult to be reproduced under the current *in vitro* testing conditions, resulting into false negative and positive responses. The present results suggest that the repeated long-term treatment of rat hepatocytes in the Collagen I-Matrigel™ sandwich configuration might be a suitable tool for safety profiling of the potential to induce phospholipidosis and impair Mrp2-mediated transport processes, but not to predict steatosis.

1. Introduction

Drug-induced liver injury (DILI) is one of the most common adverse event leading to drug attrition during pharmaceutical development (Kola and Landis, 2004) and to drug withdrawals (Wilke et al., 2007) after market introduction. There are many clinical situations and mechanisms leading to DILI. Intracellular accumulation of lipids (steatosis) or phospholipids (phospholipidosis) and inhibition of biliary clearance (cholestasis and hyperbilirubinemia) are regarded as severe pathological features affecting the liver.

Following impairment of multiple mechanisms such as mitochondrial β-oxidation, *de novo* fatty acid synthesis (lipogenesis) or fatty acid release from adipose tissues (lipolysis), neutral lipids can accumulate in hepatocytes leading to micro- and macrovesicular steatosis (Begriche et al., 2011; Labbe et al., 2008). Long-term treatment of steatotic drugs may also lead to cirrhosis and finally to liver failure (Begriche et al., 2011).

Multidrug resistance-associated protein 2 (Mrp2) is an ATP-binding cassette (ABCC2) transporter located at the bile canalicular membrane. It is a major efflux transporter involved in biliary excretion, playing a crucial role in the biliary excretion of a wide variety of organic anions, including glutathione, glutathione conjugates, sulfated and glucuronidated bile acids (Borst et al., 2006). In addition, Mrp2 plays an important role for the biliary excretion of bilirubin: the absence of Mrp2, such as in patients affected by Dubin–Johnson Syndrome (DJS) or in transport deficient (TR^-) rats, has been associated with deregulation of bilirubin homeostasis resulting into hyperbilirubinemia (Kartenbeck et al., 1996; Paulusma et al., 1996). Inhibition of Mrp2-mediated biliary clearance may result in lipid homeostasis impairment and toxic accumulation of metabolites in the hepatocytes (Tang, 2007).

Phospholipidosis (PLD) is a lysosomal storage disorder characterized by excessive accumulation of phospholipids in several tissues, such as liver, kidney and lung. Cationic amphiphilic drugs

Abbreviations: DILI, drug-induced liver injury; Mrp2, multidrug resistant protein 2; HCI, high content imaging.

* Corresponding author. Address: Discovery and Investigative Safety, Preclinical Safety, WKL-135.2.86, Novartis Institutes for Biomedical Research, Klybeckstrasse 141, CH-4057 Basel, Switzerland. Tel.: +41 61 324 1735; fax: +41 61 324 1893.
E-mail address: armin.wolf@novartis.com (A. Wolf).

http://dx.doi.org/10.1016/j.tiv.2014.05.009
0887-2333/

(CADs) have been demonstrated to possess a high potential to induce PLD (Halliwell, 1997). The impaired degradation of phospholipids by lysosomal phospholipases following CADs administration seems to be the main mechanism (Reasor and Kacew, 2001). Despite the evidence that drug-induced PLD is often reversible and that toxicological implications remain uncertain, it is still considered an adverse side effect by regulatory authorities (Berridge et al., 2007) and some challenge for pharmaceutical companies to circumvent. Therefore, the use of characterized predictive models is highly recommended in order to identify toxicity potential in preclinical phases.

Primary hepatocytes are regarded as the gold standard for assessing drug transport and metabolism *in vitro*. However, following isolation and culture, primary hepatocytes may fail to maintain their typical oriented apical and basolateral morphology as well as hepatic functions. Without embedding in an extracellular matrix, the expression and activity of cytochrome P450 (CYP) enzymes in hepatocytes cultured on plastic remains stable only during a short period. Loss of polarity can be avoided by culturing primary hepatocytes in sandwich configuration allowing longer periods of culture (Dunn et al., 1991), maintenance of liver functions (LeCluyse et al., 1994; Tuschl et al., 2009) and characteristic gene expression (Kim et al., 2010). Despite these evidences, many studies are performed between 24 and 48 h, therefore exposing the cells to a range of acute high doses not comparable to physiological concentrations. Here, a long-term culture and treatment of primary rat hepatocytes in sandwich configuration (Collagen I-Matrigel™) was used; cells could be kept in culture for 15 days and were shown to maintain typical liver functions. Regular additions of Matrigel™ layers have been found to improve significantly the quality and functions of the hepatocytes. In order to mimic a chronic treatment and to investigate the effect of 10 drugs with known adverse side effects in rats and human, cells were exposed daily to subtoxic concentrations for two weeks. The drugs were selected by the Predict-IV (FP7) consortium, a collaborative large-scale project, whose aim is to support the development of better drug testing strategies, which can be used for safety profiling of the most frequently affected target organs of toxicity (liver, kidney and CNS) (Wolf et al., 2013). Multi-parametric morphological and functional cellular responses, such as intracellular accumulation of neutral lipids and lysosomal phospholipids together with inhibition of Mrp2-mediated canalicular transport, were analyzed with the use of HCI technology, which has been shown to be a valuable tool for investigating specific drug-induced hepatotoxic events (Donato et al., 2012; McDonough et al., 2009; Tolosa et al., 2012; van de Water et al., 2011; Xu et al., 2008).

2. Materials and methods

2.1. Isolation and purification of primary rat hepatocytes

Five to six weeks old male Wistar rats were purchased from CBP Harlan. The animals had free access to food and water. Hepatocytes were isolated according to a two-step collagenase perfusion method (Paine et al., 1979; Seglen, 1976) with modifications (Paine, 1990). Briefly, rats were anaesthetized with an intraperitoneal injection of sodium pentobarbitone (75 μg/g body weight). Liver perfusion was performed through the portal vein with Ca^{2+}/Mg^{2+}-free pre-perfusion buffer (0.5 mM EGTA (Fluka) supplemented with 10 mM HEPES-buffered Hanks' balanced salt solution (Invitrogen)) at a constant flow rate of 25 ml/min. After 7–8 min the pre-perfusion solution was replaced by the perfusion buffer (DMEM/F12 (Gibco) supplemented with 0.3 M $CaCl_2$ (Sigma), 1 M HEPES (Gibco), 1% Pen/Strep/Glut (Invitrogen) containing, and 100 U/ml collagenase A (Roche)) at decreasing flow rates from 25 to 12 ml/min. After additional 8–10 min perfusion, the liver was dissected and manually dissociated in 25 ml collagenase buffer. The resulting cell suspension was filtered through a 100 μm gauze into a 50 ml plastic tube and then filled with cold wash buffer (DMEM/F12 supplemented with 20% FCS (HyClone), 1 M HEPES, 1% Pen/Strep/Glut). Parenchymal cells were separated from the previous cell suspension by two cycles of low-speed centrifugation (50 g, 5 min, 4 °C). The supernatant was discarded and the cells were then re-suspended in 25 ml of attachment medium (Williams' Medium E supplemented with 10% FCS, 10 mM HEPES, 0.17 μM insulin (Sigma), 0.3 μM dexamethasone (Sigma), 1% Pen/Strep/Glut) and added to a Percoll gradient (Percoll™ Plus (GE Healthcare), HBSS 10X (Gibco), 1 M HCl). After 10 min spinning (50 g, 4 °C) the cells were re-suspended and washed in attachment medium before viability determination by Trypan Blue. Hepatocytes preparations with viability greater than 85% were used for cultivation.

2.2. Cell culture and long-term treatments

Hepatocytes were seeded (3.5×10^5 cells/well) on 24-well collagen I-coated plates (BD Biocoat). After 2–3 h, non-attached cells were removed and a top layer of Matrigel™ (250 μg/ml; BD #356237) diluted in serum-free medium (DMEM/F12 supplemented with sodium pyruvate (Gibco), 1X Insulin/Transferrin/Selenium (Gibco), 0.03 μM dexamethasone, 1% Pen/Strep, albumin solution from bovine serum (Sigma)) was applied with pre-cooled pipette. Medium was changed every 24 h. Hepatocyte morphology was monitored daily. Other layers of Matrigel™ were added at day 4 and 8 and 12 of culture. For selected experiments rat hepatocytes were cultured in presence of DMEM/F12 supplemented with Recombinant Human Epidermal Growth Factor (hEGF, Invitrogen) or 0.5% FCS and with HCM™ Bullet Kit (Hepatocyte Culture Medium, Lonza). The following compounds chosen from a training set used in the 7th EU Framework project Predict-IV were used for the long-term term treatment: Cyclosporin A, Metformin (Calbiochem, Switzerland); Rosiglitazone, Troglitazone (Cayman Chemicals, USA); Amiodarone, Chlorpromazine hydrochloride, Fenofibrate, Ibuprofen, Acetaminophen, Valproic Acid sodium salt (Sigma–Aldrich, Germany). Non-cytotoxic concentrations were chosen (Table 2) and rat hepatocytes were exposed 14 days to perform chronic treatment. The treatments started 24 h after cell seeding. All compounds were dissolved in DMSO and added to the medium with a final concentration of 0.1% vol/vol DMSO. Cells incubated in the presence of 0.1% vol/vol DMSO were used as control.

2.3. Biochemical assays

ATP assay: ATP was measured with CellTiter-Glo® Luminescent Cell Viability Assay (Promega, USA) according to manufacturer's instructions.

Lactate Dehydrogenase (LDH) release: LDH release was measured with Cytotoxicity Detection Kit^{Plus} (Roche, Germany) according to manufacturer's instructions.

Urea synthesis: Urea synthesis was measured with Biochain's Urea Assay Kit (Biochain, USA) according to manufacturer's instructions.

Albumin secretion: Albumin content was assessed with Rat Albumin ELISA Quantitation Set (Bethyl Laboratories (Montgomery, TX, USA) according to the manufacturer's instructions.

2.4. Microscopy imaging and analysis and functional assays

All fluorescence microscopy images of were taken with Thermo Scientific Cellomics™ Arrayscan® VTI, with XF93 Hoechst, FITC, TRITC excitation/emission filters and 10×/20× objective. An amount of at least 2000 cells per well were imaged (8–10

Table 1
Primers used in Real-Time Polymerase Chain Reaction.

Gene symbol	Gene name	Alias	RefSeq	Amplicon length
Abcb11	ATP-binding cassette, sub-family B (MDR/TAP), member 11	Bsep	NM_031760.1	75
Abcb1b	ATP-binding cassette, sub-family B (MDR/TAP), member 1B	Mdr1	NM_012623.2	66
Abcc1	ATP-binding cassette, sub-family C (CFTR/MRP), member 1	Mrp1	NM_022281.2	87
Abcc2	ATP-binding cassette, sub-family C (CFTR/MRP), member 2	Cmoat Mrp2	NM_012833.1	78
Abcc3	ATP-binding cassette, sub-family C (CFTR/MRP), member 3	Mrp3	NM_080581.1	63
Abcc4	ATP-binding cassette, sub-family C (CFTR/MRP), member 4	Mrp4	NM_133411.1	70
Slco1a1	Solute carrier organic anion transporter family, member 1a1	Oatp1 Oatp1a1	NM_017111.1	80
Slco1a4	Solute carrier organic anion transporter family, member 1a4	Oatp2 Oatp1a4	NM_131906.1	134
Slco1b2	Solute carrier organic anion transporter family, member 1b2	Oatp4 Oatp1b2	NM_031650.1	83
Cyp3a2	Cytochrome P450, family 3, subfamily a, polypeptide 2	Cyp3a11	NM_153312.2	116
Cyp7a1	Cytochrome P450, family 7, subfamily a, polypeptide 1	CHAP CYP7 CYP7S1	NM_012942.1	81
Nr1h4	Nuclear receptor subfamily 1, group H, member 4	Fxr	NM_021745.1	95
Nr1i3	Nuclear receptor subfamily 1, group I, member 3	CAR	NM_022941.3	63
Nr1i2	Nuclear receptor subfamily 1, group I, member 2	PXR	NM_052980.2	59
Gapdh	Glyceraldehyde-3-phosphate dehydrogenase	Gapd	NM_017008.3	87

images/well with a 10× objective; 15–20 images/well with a 20× objective). Fluorescence intensities were quantified by using Spot Detector and Compartmental Analysis BioApplication calculating the sum of average fluorescence intensity within a ring surrounding nuclei with a radius of 15 μm for each cell, followed by division of total number of cells measured.

Mrp2-mediated transport measurement: Cells were washed twice and incubated with pre-warmed HBSS (+Ca^{2+}/Mg^{2+}) 10 min at 37 °C. Next, cells were stained with Hoechst 33,342 (10 μg/ml) and 5-(and-6)-carboxy-2′,7′-dichlorofluorescein diacetate (carboxy-DCFDA) (4 μM in DMSO) (Invitrogen, USA) to assess Mrp2-mediated biliary transport and incubated 15 min at 37 °C. The images acquired with Cellomics™ Arrayscan® were analyzed by Spot Detector V4 BioApplication.

Neutral lipid accumulation: Cells were washed twice with HBSS (+Ca^{2+}/Mg^{2+}), stained with Hoechst 33,342 and BODIPY® 493/503 (4,4-difluoro-1,3,5,7,8-pentamethyl-4-bora-3a,4a-diaza-s-indacene) (2 μM in DMSO) (Invitrogen, USA) and incubated 15 min at 37 °C. The images acquired with Cellomics™ Arrayscan® were analyzed by Compartmental Analysis V4 BioApplication.

Phospholipids accumulation: Cells were washed twice with HBSS (+Ca^{2+}/Mg^{2+}) and stained HCS LipidTox™ Red (1:1000 in culture medium) (Invitrogen, USA) for 24 h at 37 °C in culture medium. After 24 h, the cells were washed 3 times with HBSS (+Ca^{2+}/Mg^{2+}), stained with Hoechst 33,342 and incubated 10 min at 37 °C. The images acquired with Cellomics™ Arrayscan® were analyzed by Spot Detector V4 BioApplication.

2.5. Real time–PCR (RT–PCR)

FastLane Cell Multiplex Kit (200), (Qiagen, USA) was used to isolate first-strand cDNA directly from cultured cells without RNA purification according to manufacturer's instructions. RT–PCR was performed using a StepOnePlus™ Instrument (Applied Biosystems, USA) in the presence of TaqMan® Gene E probes (Table 1) (Applied Biosystems, USA). Glyceraldehyde-3-phosphate dehydrogenase (GAPDH) was used as internal control. A volume of 20 μl was the used for each reaction. Relative gene expression was analyzed using the $2^{-\Delta\Delta Ct}$ method.

2.6. Statistics

Statistical comparisons were performed between each dose group and the control using two-way ANOVA. Values were first normalized within each experiment in percent of control, to make the experiments comparable. The data were obtained from 3 independent experiments, each of them consisting of 3 replicates. Statistical analysis was conducted using Graph Pad Prism 6 software. Differences compared to respective daily controls were considered as statistically significant for $^{*}p < 0.05$.

3. Results

3.1. Improved cellular morphology and functionality by addition of multiple Matrigel™ layers

Following isolation, primary rat hepatocytes were purified and cultured in Collagen I-coated plates. After the addition of a layer of Matrigel™, hepatocytes showed typical cuboidal morphology within the same day (Fig. 1A), whereas the canalicular networks were visible only after 2–3 days in culture (Fig. 1B). After 8 days in culture rat hepatocytes started to lose their cuboidal morphology and acquired spindle-like shape (Fig. 1C and D) together with dead cell detachment from the wells (Fig. 1E). In contrast, cells receiving a second layer of Matrigel™ on day 7 showed significant improvement of the culture quality. The cells maintained their morphology together with a lower disruption of the canalicular networks after 8 days (Fig. 1H–J).

In order to investigate whether the addition of further layers of Matrigel™ would further improve the quality and the functional properties of the hepatocytes, 3 (day 0, 5 and 10) or 4 layers (day 0, 4, 8 and 12) were added over a period of 14 days. No significant differences in terms of intracellular ATP and LDH release were observed between day 1 and day 14 (Fig. 2A and B). The functionality of hepatocytes was investigated at day 14 of culture by incubation of carboxy-DCFDA, a dye cleaved by cytosolic esterases resulting in the formation of dichlorofluorescein (DCF), which is then transported specifically by the canalicular transporter Mrp2 (Zamek-Gliszczynski et al., 2003). The number of cells, regarded as valid objects, as well as the spot average area and intensity of the fluorescent signal within the object, were chosen as parameters and illustrated in Fig. 2C–E. As shown in Fig. 2F–H, DCF accumulated in the canaliculi, confirming that hepatocytes cultured in our conditions maintained their functional Mrp2 transporter activity. The intensity of fluorescent signal was lower in the canaliculi of adjacent hepatocytes cultured with 2 layers only (Fig. 2F), compared to cells receiving 4 layers of Matrigel™ (Fig. 2H). Analysis

Table 2
Summary of *in vitro* results compared with preclinical/clinical C_{max} and observed side effects. 0.1% DMSO was used as vehicle control.

Effects observed in liver									
	In vitro					*In vivo*			
Compounds and Concentrations (μM)	Endpoints	Lowest effective concentration (μM)				Preclinical		Clinical	
		Day 3	Day 7	Day 10	Day 14	C_{max} (μM)	Side effects	C_{max} (μM)	Side effects
Cyclosporin A (CsA) (0.3, 1, 3)	Mrp2 inhibition ↓	3	1	1	1	(0.96–2.3) (Guan et al., 2011; Ishizaki et al., 2008)	Cholestasis (Stone et al., 1987), Hyperbilirubinemia (Roman et al., 1990)	(0.44–1.39)[#]	Cholestasis (Myara et al., 1996), Hyperbilirubinemia (Ertorer et al., 1997)
	Neutral Lipids ↑	3	1	0.3	0.3				
	Phospholipids ↑								
	ATP ↓			3	1				
	LDH ↑			3	1				
Amiodarone (AMD) (1, 2.5, 5)	Mrp2 inhibition ↓					(0.6–2.14) (Fruncillo et al., 1985; Rodrigues et al., 2012)	Phospholipidosis (Halliwell, 1997)	(2.32–3.72)[#]	Phospholipidosis (Poucell et al., 1984)
	Neutral Lipids ↑								
	Phospholipids ↑	5	5	5	2.5				
	ATP ↓								
	LDH ↑			5	5				
Rosiglitazone (RGZ) (10, 20, 50)	Mrp2 inhibition ↓					(1.33–33.52) (Lakshmi and Rajesh, 2011; Varanasi et al., 2008)	Mitochondrial impairment (Feinstein et al., 2005)	(1.35–2)[#]	Hepatocellular damage (Floyd et al., 2009)
	Neutral Lipids ↑				50				
	Phospholipids ↑								
	ATP ↓								
	LDH ↑				50				
Chlorpromazine (CPZ) (1, 5, 10)	Mrp2 inhibition ↓	1	5	1	5	(0.03–0.2) (Imamura et al., 1988; Zhang et al., 2007)	Cholestasis (Barth et al., 1978), Hyperbilirubinemia (Obata, 1983), Phospholipidosis (Hirode et al., 2008)	(0.07–0.42)[#]	Cholestasis (Regal et al., 1987), Hyperbilirubinemia (Waitzkin, 1962), Phospholipidosis (Halliwell, 1997)
	Neutral Lipids ↑								
	Phospholipids ↑		10						
	ATP ↓								
	LDH ↑			5	10				
Troglitazone (TGZ) (5, 10, 25)	Mrp2 inhibition ↓	5	10	10	25	(2.04–6.39) (Loi et al., 1999)	Cholestasis (Funk et al., 2001a)	(2.04–6.32)[#]	Cholestasis (Menon et al., 2001)
	Neutral Lipids ↑								
	Phospholipids ↑								
	ATP ↓								
	LDH ↑								

Metformin (MET) (10, 25, 50)	Mrp2 inhibition ↓ Neutral Lipids ↑ Phospholipids ↑ ATP ↓ LDH ↑	50		(15.81–83.92) (Choi et al., 2010; Lal and Jain, 2010)		(6.04–18.72)[#]		
Fenofibrate (FFB) (5, 10, 25)	Mrp2 inhibition ↓ Neutral Lipids ↑ Phospholipids ↑ ATP ↓ LDH ↑	25	25	(2.27–9.83) (Li et al., 2009)		(21.33–31.59)[#]		
Ibuprofen (IBU) (10, 20, 50)	Mrp2 inhibition ↓ Neutral Lipids ↑ Phospholipids ↑ ATP ↓ LDH ↑	50	50	(25.74–129.91) (Khan and Akhter, 2005; Newa et al., 2008)		(269.5–322.85)[#]		
Acetaminophen (ACT) (250, 500, 1000)	Mrp2 inhibition ↓ Neutral Lipids ↑ Phospholipids ↑ ATP ↓ LDH ↑			(80.31–365.81) (Yamamoto et al., 2007; Yamasaki et al., 2011)	ALT/AST increase, hepatocellular damage (Gardner et al., 1998)	(132.3)[#]	ALT/AST increase, Hepatocellular damage (Bolesta and Haber, 2002)	
Valproic Acid (VPA) (10, 20, 50)	Mrp2 inhibition ↓ Neutral Lipids ↑ Phospholipids ↑ ATP ↓ LDH ↑			(566.82–1292.86) (Blotnik et al., 1996; Ohshiro et al., 2003)	Mitochondrial impairment (Tong et al., 2005), Steatosis (Lewis et al., 1982)	(180.29–291.24)[#]	Mitochondrial impairment (Finsterer and Zarrouk, 2012), Steatosis (Zimmerman and Ishak, 1982)	

[#] Human C_{max} values were extrapolated from Goodman & Gilman's. The pharmacological basis of therapeutics, 12e.

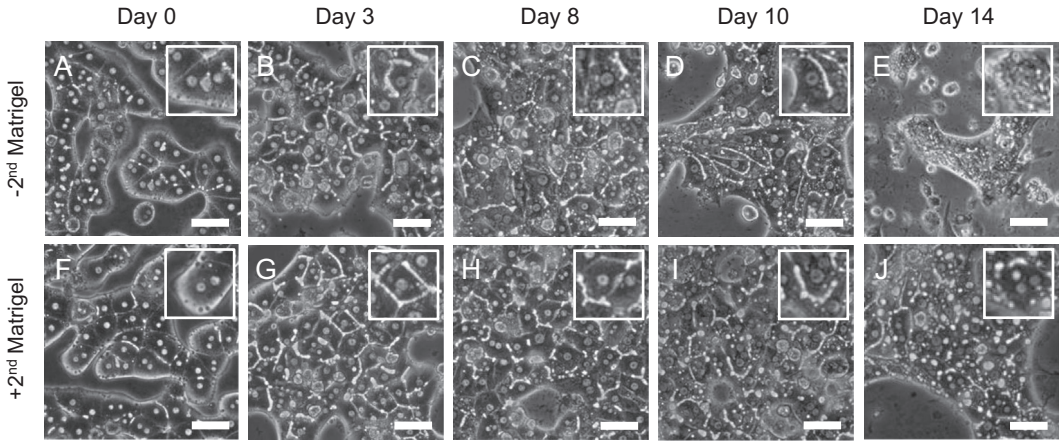

Fig. 1. Morphological differences of rat hepatocytes in presence or absence of second layer of Matrigel™. Representative phase contrast images of rat hepatocytes cultured with single (A–E) or double addition of Matrigel™ top layer (F–J) at selected timepoints. Bar = 50 μm.

of scanned images confirmed that the average intensity and the average area of fluorescent signal were significantly higher in hepatocytes cultured with 4 layers of Matrigel™ (Fig. 2D and E). In addition, the number of viable cells was higher with increasing number of the layers of Matrigel™ applied (Fig. 2C). Based on these findings, all hepatocyte experiments were performed in cultures with 4 layers of Matrigel™.

The analysis of supernatants collected at different timepoints displayed the maintenance of specific functions such as albumin secretion (Fig. 3A) and urea synthesis (Fig. 3B) over 14 days of culture. Moreover, the expression of specific genes at several timepoints (day 1, 3, 7, 10, and 14) was assessed by RT–PCR. As shown in Fig. 3C, the expression of hepatocyte specific genes such as canalicular and sinusoidal transporters was stable and maintained over the whole period of culture, as well as the expression of nuclear receptor and CYPs.

3.2. Evaluation of drug-induced effects after 14 days repeated treatments

The chronic-like toxicity of 10 selected compounds was investigated by daily repetitive treatment for 14 days. The concentrations

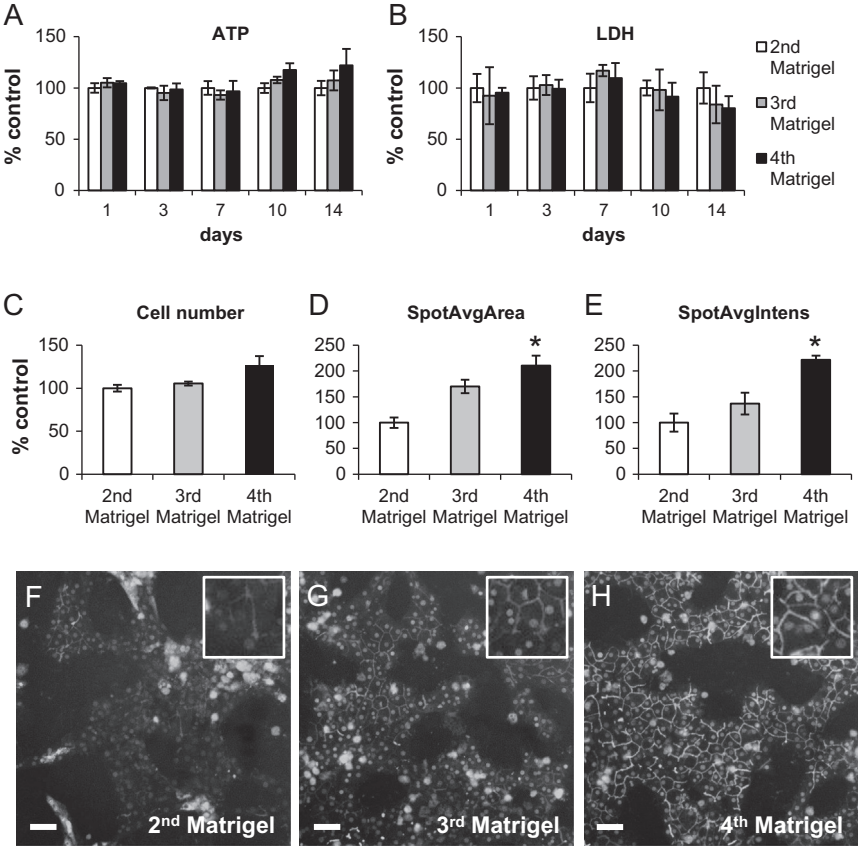

Fig. 2. Influence of multiple layers of Matrigel™ on rat hepatocytes cultures. Comparison of intracellular ATP (A) and LDH release (B). To measure canalicular transport, cells were incubated with carboxy-DCFDA. Fluorescent signal of DCF was quantified with Spot Detector V4 BioApplication (C–E). Representative images of Mrp2-mediated DCF accumulation in canaliculi of rat hepatocytes cultured in presence of two (F), three (G) or four (H) layers of MatrigelTM. Original magnification: 10×. ($n = 3$; $^{*}p < 0.05$). Bar = 50 μm. Error bars represent standard deviation ($n = 3$).

selected for the 14-day long-term treatments derived from 48-h cytotoxicity studies. Three non-cytotoxic concentrations for 48-h incubation were chosen (low, middle, high) for each compound. The highest non-cytotoxic concentration during 48 h, as measured by cellular viability (ATP) and cellular leakage (LDH), was selected as the high dose for the 14-day treatments (Suppl. Fig. 2). Non-cytotoxic concentrations were chosen in order to observe and identify specific responses in absence of overt cell death due to unspecific mechanisms. Table 2 illustrates the list of compounds and concentrations used for the long-term treatments. HCI was used to measure endpoints associated with liver pathological or mechanism-based features. Inhibition of Mrp2-mediated canalicular transport, intracellular accumulation of neutral lipids in the cytoplasm (steatosis) and accumulation of phospholipids in organelles of lysosomal origin were evaluated with specific fluorescent dyes. Cell number, also monitored over 14 days of treatment, was not affected by any of the compounds (*data not shown*). On day 1, none of the selected compounds did induce significant changes in any of the investigated endpoints and thus were not included in the following illustration of results.

CsA was daily administered at concentrations of 0.3, 1 and 3 μM for 14 days. On day 1, 3, 7, 10 and 14, samples were investigated for the selected endpoints. Morphological investigations revealed that the 3 μM CsA exposure resulted into accumulation of vacuoles within the cytoplasm associated with minimal loss of hepatic morphology on day 3 (Fig. 4D). An increased number of vacuoles and disruption of canalicular network was observed after 14 days (Fig. 4P). The presence of vacuoles was visible already at the lower concentrations from day 7 (Fig. 4G, J, N, O).

Further biochemical investigations are shown in Fig. 5A. The intracellular ATP levels were not affected within the first days of culture, but decreased only after 14 days of treatment with CsA at the concentrations of 1 μM ($^{*}p < 0.05$) and 3 μM ($^{**}p < 0.01$) Accordingly, LDH levels increased at day 14 at both 1 μM ($^{*}p < 0.05$) and 3 μM CsA concentrations ($^{**}p < 0.01$). In contrast, CsA affected the Mrp2-mediated canalicular transport already after 3 days of exposure at 3 μM ($^{****}p < 0.0001$). The inhibition occurred in a time- and concentration-fashion and resulted in a 54% spot average intensity decrease at 0.3 μM ($^{****}p < 0.0001$) and 76% decrease at 1 μM CsA on day 14. Images confirmed that partial inhibition of Mrp2-mediated canalicular transport occurred already after 3 days at 3 μM dose (Suppl. Fig. 3D). This resulted into a reduced quantification of fluorescent signal, as displayed by the cyan spots overlaying with the DCF (Suppl. Fig. 3H). As a consequence of the reduced export of DCF, a clear retention of the dye within the cytoplasm was observed; such effect was exacerbated after 14 days of treatment (Suppl. Fig. 3N–P). The effect of CsA on lipid metabolism was evaluated by reagents staining respectively neutral lipids and phospholipids. As shown in Fig. 5A, the accumulation of neutral lipids was detected already after 3 days of treatment (3 μM, $^{**}p < 0.01$). The size of intracellular vacuoles increased over the time of treatment (Suppl. Fig. 4). On contrast, CsA exposure did not affect the amount of phospholipids.

Exposure to AMD did not affect intracellular ATP levels, but affected LDH levels at late stages of treatment (day 10 and 14) at the highest drug concentration only (5 μM, $^{*}p < 0.05$) (Fig. 5B). AMD treatment was associated with increase of phospholipids content already after 3 days at a concentration of 5 μM ($^{*}p < 0.05$), resulting in significant changes after 14 days at concentrations of 2.5 μM ($^{*}p < 0.05$) as well as a at 5 μM ($^{***}p < 0.001$) (Images taken at day 3 and 14 (Suppl. Fig. 5) displayed the increase of phospholipids in hepatocytes treated with AMD. Increased fluorescence signal reflecting the accumulation of phospholipids was observed at 5 μM concentrations (Fig. Suppl. Fig. 5L and P), as compared to vehicle control (Suppl. Fig. 5I and M).

LDH release following CPZ exposure was found only at day 14 of treatment (5 μM, $^{**}p < 0.01$; 10 μM, $^{*}p < 0.05$) (Fig. 6B), whereas Mrp2-mediated canalicular transport was reduced at day 3 at all

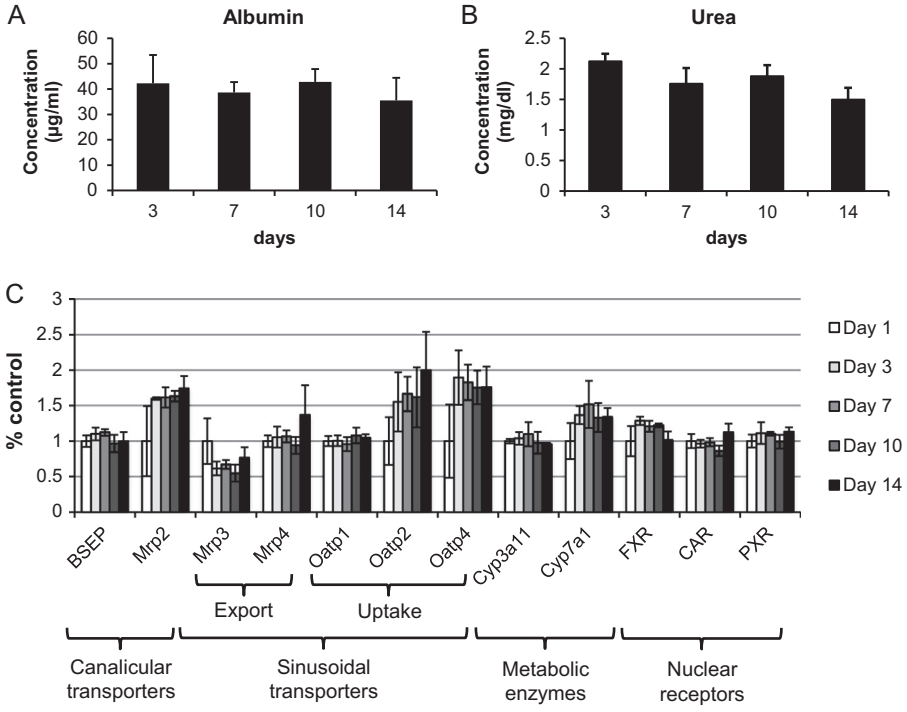

Fig. 3. Characterization of 4-layer Matrigel™ culture. Supernatants collected from rat hepatocytes sandwich cultures at different timepoints display maintenance of specific functions such as albumin secretion (A) and urea synthesis (B). Real Time PCR analysis of long-term culture showing stable expression of hepatocyte specific genes over the whole period of culture (C). Error bars represent standard deviation ($n = 3$).

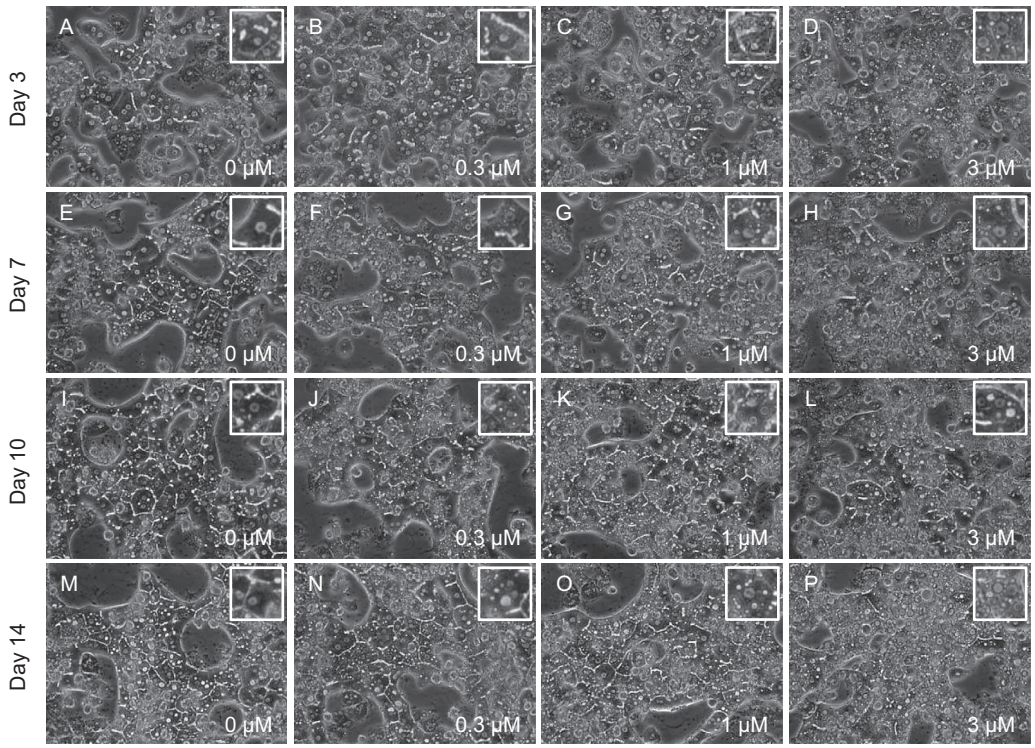

Fig. 4. Treatment of rat hepatocytes with CsA for 14 days. Representative images of 0.1% DMSO vehicle control-treated (A, E, I, M) versus CsA-treated hepatocytes at 0.3 μM (B, F, J, N) 1 μM (C, G, K, O) and 3 μM (D, H, L, P) concentrations at selected timepoints. Original magnification: 20×.

concentrations used (1 μM, $^{*}p < 0.05$; 5 μM and 10 μM, $^{****}p < 0.0001$). In addition, 10 μM CPZ enhanced the content of intracellular phospholipids after 7 and 14 days ($^{*}p < 0.05$).

Similarly, treatment of rat hepatocytes with TGZ resulted into inhibition of canalicular transport after 3 days at all concentrations (5 μM, $^{*}p < 0.05$; 10 μM, $^{***}p < 0.001$; 25 μM, $^{***}p < 0.001$) (Fig. 7A), whereas no cytotoxicity was observed over 14-day exposure.

Exposure of RGZ resulted into accumulation of neutral lipids by day 14 at the highest concentration (50 μM, $^{*}p < 0.05$) (Fig. 6A; Suppl. Fig. 6K, L, Q and P) which was associated at the same time with increased leakage of LDH.

Cells treated with ACT and VPA did not display any sign of cytotoxicity (Fig. 9A and B). In addition canalicular transport and lipid metabolism were not affected. MET 50 μM (Fig. 7B), FFB 25 μM (Fig. 8A) and IBU 50 μM (Fig. 8B) treatments were only associated with LDH release at day 10 and 14.

4. Discussion

The data presented here illustrate further improvement of the rat hepatocyte Collagen I-Matrigel™ sandwich *in vitro* model, where primary rat hepatocytes were maintained in a functional state for a period of 14 days. The addition of multiple layers of Matrigel™ has been demonstrated to be a robust method for the maintenance of hepatocyte morphology and specific functions. Mrp2-mediated transport quantified by HCI was enhanced when hepatocytes received 4 layers of Matrigel™ over 2 weeks of culture. In these conditions, the expression of liver specific genes, such as transporters, nuclear receptor and CYPs was stable over the whole culture duration. However, in this setting the addition of a low percentage of serum as well as the presence of EGF in the cell culture medium did not improve the cells status, despite some published evidences showing enhancement of long-term maintenance and survival of rat hepatocytes (Farkas and Tannenbaum, 2005). (Suppl. Fig. 1B and F).

These culture conditions allowed mimicking chronic treatment by multiple exposures of hepatocytes to different hepatotoxicants. By combining a stable and reproducible *in vitro* culture system exposed daily to low non-cytotoxic concentrations for 14 days together with HCI technology, specific cellular responses associated with liver pathological features could be monitored and quantified.

In some instances, drug withdrawals from market were the result of "Hy's law" cases, indicated by a 2-fold bilirubin increase with a concomitant occurrence of 3-fold ALT increase in plasma. These combined events are admitted as a high risk of fatal liver failure. After being formed in the systemic circulation, bilirubin is transported into the hepatocytes, metabolized to give diglucuronide metabolite and excreted into the bile by Mrp2. Mrp2 (ABCC2) is also known to mediate the biliary excretion of glutathione and sulfate metabolites. Mrp2 impairment can affect the hepatic clearance of endogenous compounds, such as steroids, leukotrienes and many clinically important drugs (Gerk and Vore, 2002). The clinical importance of Mrp2-inhibition has been demonstrated by Mrp2 gene mutations (Kartenbeck et al., 1996) as well as by the down-regulation of its expression (Terui et al., 2011; Yamada et al., 2005) and its association with the occurrence of hyperbilirubinemia. Hence, it is of importance to dispose of an assay to avoid drug inhibition of Mrp2. The present data show that the exposure of rat hepatocytes to CsA, CPZ and TGZ resulted into the inhibition of Mrp2-mediated transport of DCF in a dose- and time-dependent manner. A reduction of fluorescent signal in the canaliculi followed by accumulation of the fluorescent dye into the cytoplasm was the result of Mrp2 inhibition. These effects were shown to occur already after 3 days of treatment, whereas cytotoxicity was observed only after 10 days of exposure. Side effects of the immunosuppressive drug CsA are

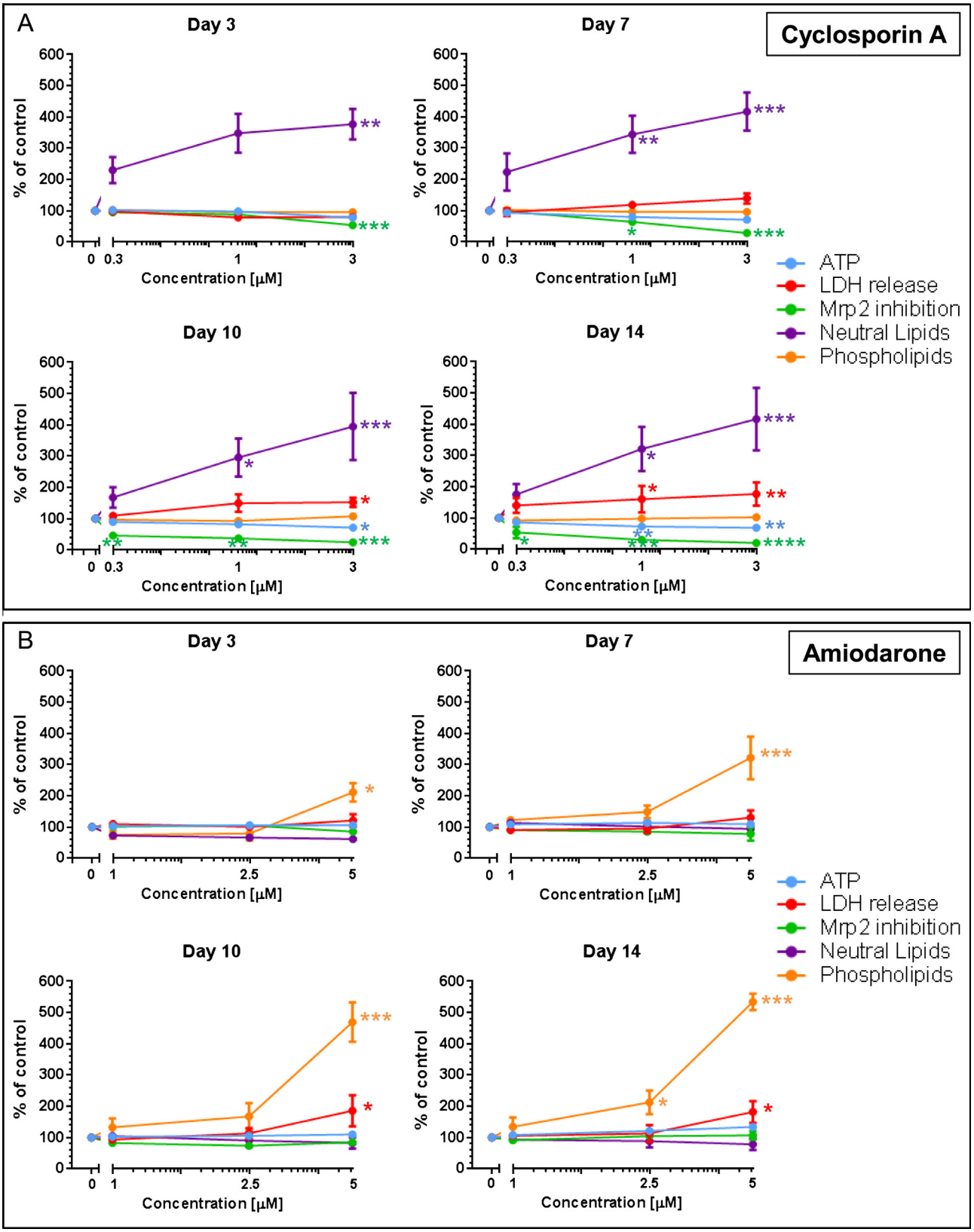

Fig. 5. Graphs showing the effects of CsA (A) and AMD (B) on inhibition of Mrp2-mediated canalicular transport, accumulation of neutral lipids and phospholipids, intracellular ATP and LDH release. Error bars represent standard error ($^{*}p < 0.05$, $^{**}p < 0.01$, $^{***}p < 0.001$, $^{****}p < 0.0001$; two-way ANOVA).

ranging from renal, neuronal to hepatic adverse side effects in animals and man (Kahan, 1989; Wiesner et al., 1990). The most common abnormalities related to hepatotoxicity are increases of serum bile salt levels, cholestasis (Kahan, 1989; Myara et al., 1996) and hyperbilirubinemia (Ertorer et al., 1997). Mrp2, together with BSEP and MDR1, are ATP-dependent transporters

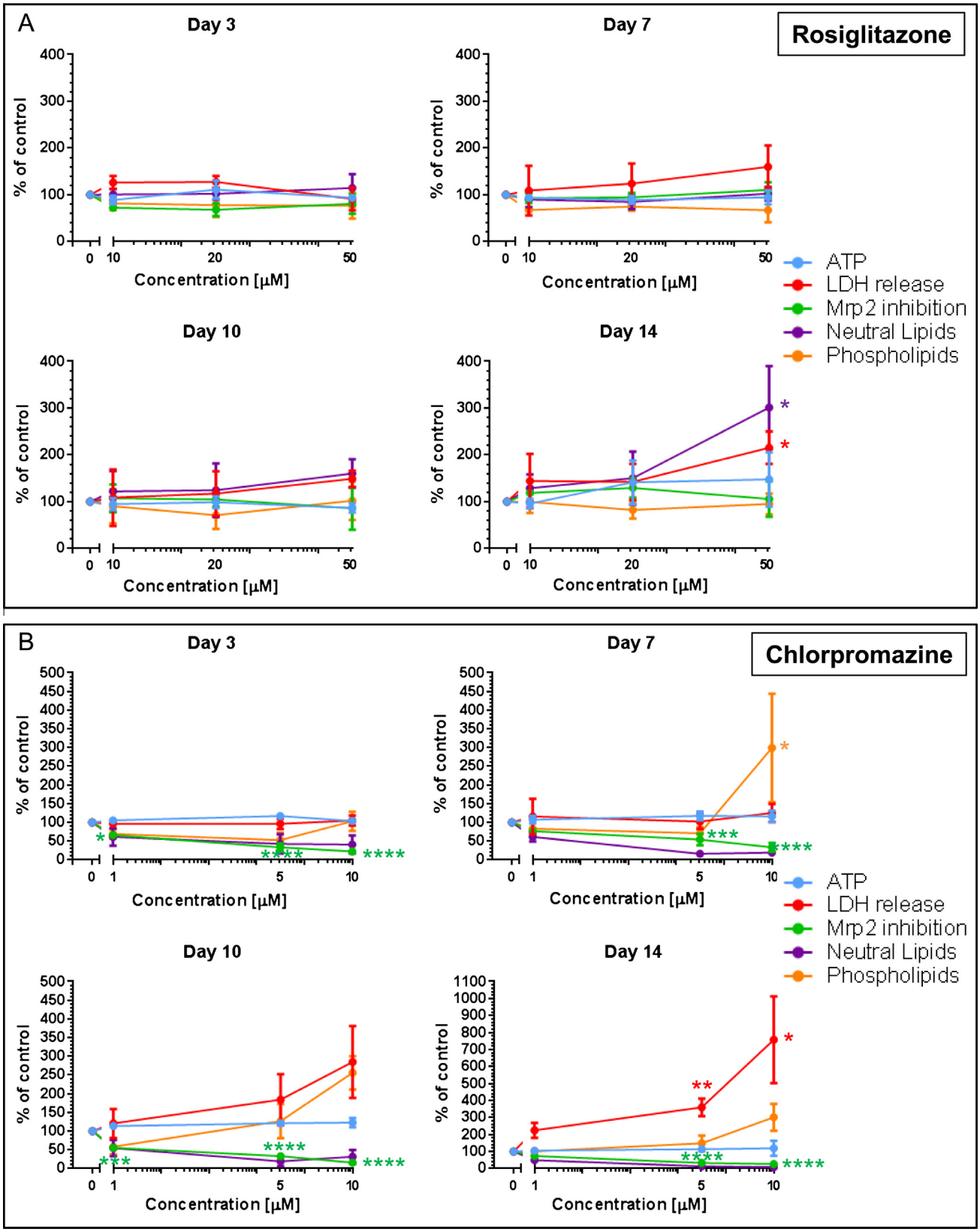

Fig. 6. Graphs showing the effects of RGZ (A) and CPZ (B) on inhibition of Mrp2-mediated canalicular transport, accumulation of neutral lipids and phospholipids, intracellular ATP and LDH release. Error bars represent standard error (*$p < 0.05$, **$p < 0.01$, ***$p < 0.001$, ****$p < 0.0001$; two-way ANOVA).

known to be inhibited by CsA (Bohme et al., 1993; Kahan, 1989; Kobayashi et al., 2004). TGZ has been shown to decrease Mrp2 expression in liver (Foster et al., 2012), whereas CPZ has been shown to inhibit directly Mrp2-mediated transport of estradiol-17-β-glucuronide (Pedersen et al., 2008). Other studies suggested that an imbalance of intracellular ATP might occur following CsA,

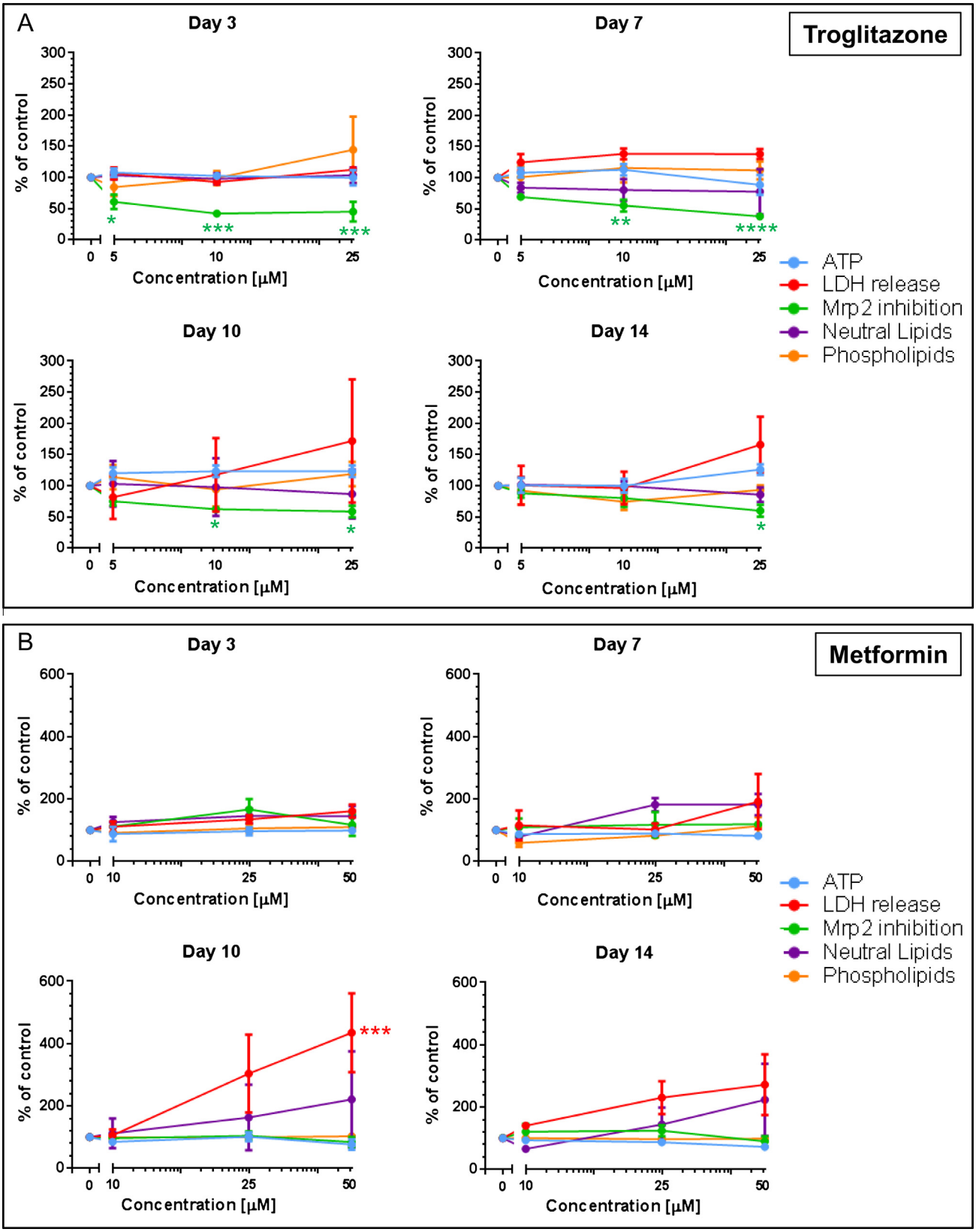

Fig. 7. Graphs showing the effects of TGZ (A) and MET (B) on inhibition of Mrp2-mediated canalicular transport, accumulation of neutral lipids and phospholipids, intracellular ATP and LDH release. Error bars represent standard error ($^{*}p < 0.05$, $^{***}p < 0.001$; two-way ANOVA).

CPZ and TGZ treatment, leading to a reduction of ATP-dependent canalicular transport of bile salts in the liver (Ballantyne et al., 1989; Funk et al., 2001; Samuels and Carey, 1978; Ziegler and Frimmer, 1986). However, changes in the content of ATP during early stages were not observed here, suggesting that additional mechanisms must be involved.

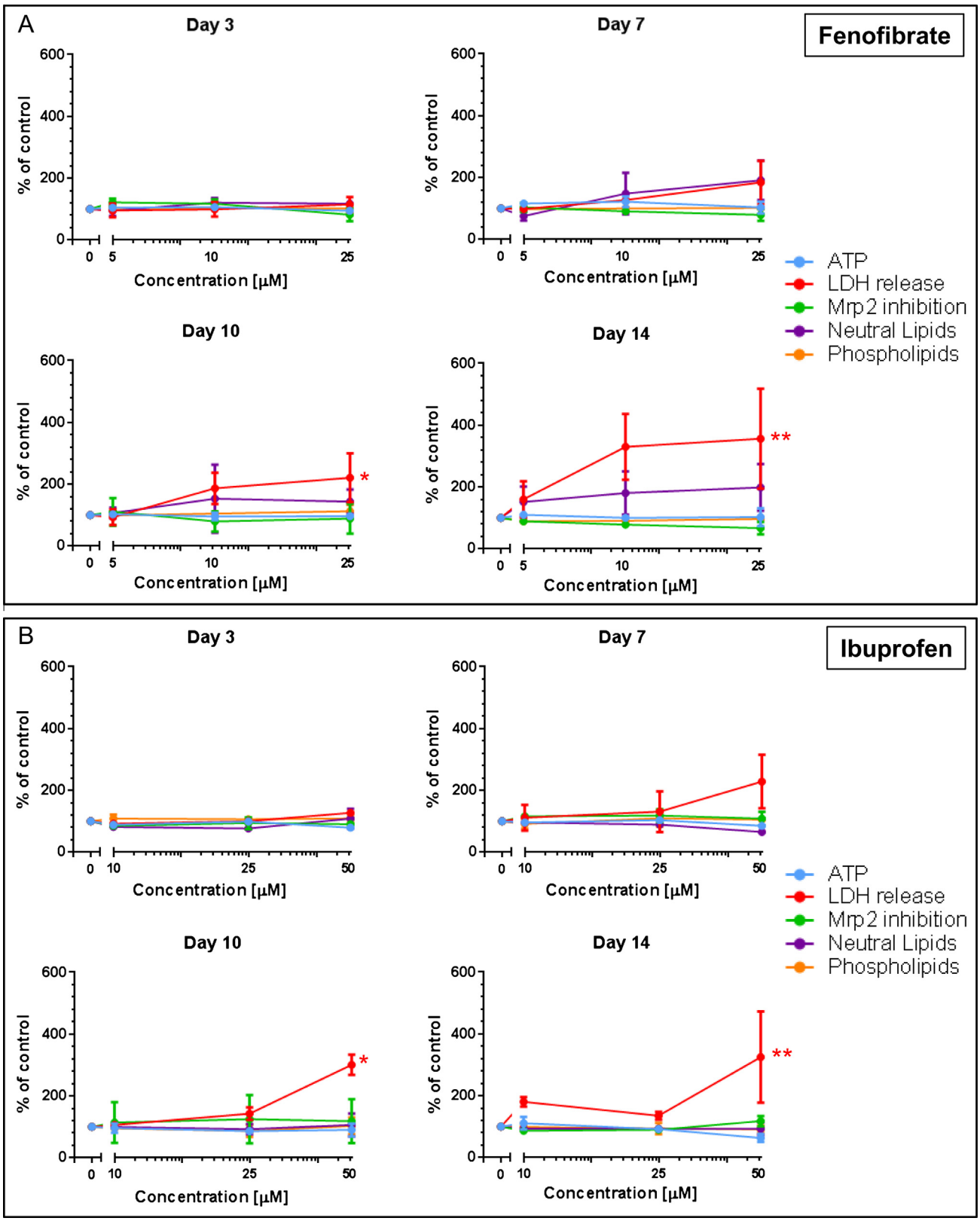

Fig. 8. Graphs showing the effects of FFB (A) and IBU (B) on inhibition of Mrp2-mediated canalicular transport, accumulation of neutral lipids and phospholipids, intracellular ATP and LDH release. Error bars represent standard error ($^{*}p < 0.05$, $^{**}p < 0.01$; two-way ANOVA).

AMD is an antiarrhythmic drug being reported, among several other cationic amphiphilic drugs such as CPZ, to induce PLD (Halliwell, 1997). Both drugs are regarded as inhibitors of phospholipase activity and therefore impairing phospholipid catabolism (Shaikh et al., 1987). While PLD does not constitute overt toxicity *per se*, it has been reported to be associated with drug or metabolite accumulation in affected tissues (Hruban, 1984), and as such, possibly contributing to untoward side effects. In addition,

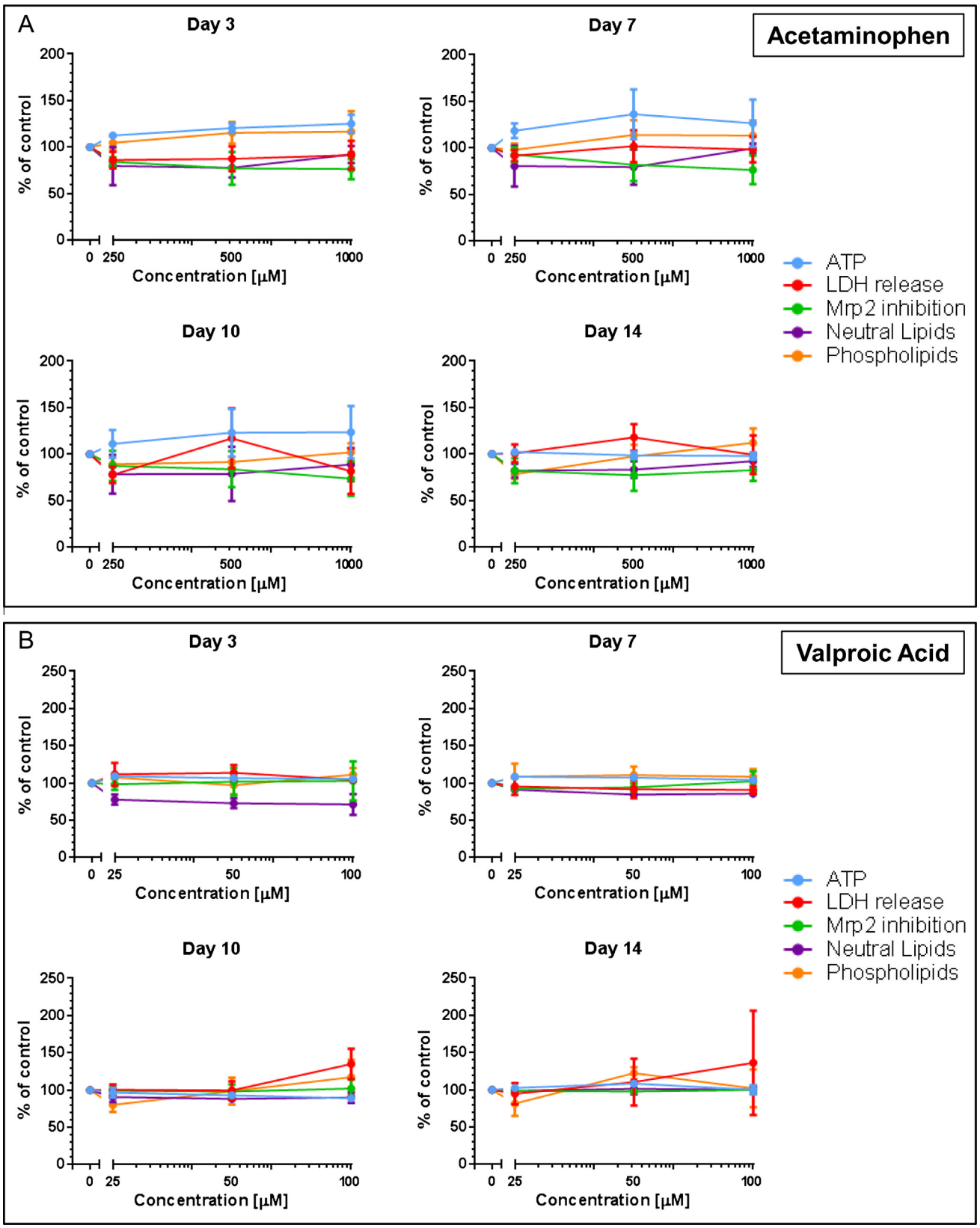

Fig. 9. Graphs showing the effects of ACT (A) and VPA (B) on inhibition of Mrp2-mediated canalicular transport, accumulation of neutral lipids and phospholipids, intracellular ATP and LDH release. Error bars represent standard error.

a case of liver cirrhosis in a patient chronically treated with AMD, associated with PLD has been reported (Oikawa et al., 2005). The treatment of rat hepatocytes with AMD and CPZ at low concentrations did not cause cytotoxicity. Increase of LDH was observed in the supernatant of hepatocytes treated only with higher concentrations at day 14 of culture (AMD 5 µM, CPZ 5 and 10 µM). On

the other hand, the HCI investigations revealed a strong accumulation of phospholipids already after few days and increased over time in a concentration-dependent fashion. These observations were in line with several studies reporting occurrence of PLD *in vivo* (Hirode et al., 2008; Lewis et al., 1990) and *in vitro* (Fujimura et al., 2007; Kuroda and Saito, 2010; Morelli et al., 2006; Schurdak et al., 2007) detected with cell-based fluorescence assays.

The investigation of steatosis displayed false negative and false positive results: the data generated *in vitro* were not correlating with *in vivo* findings. CsA, which has never been reported to induce steatosis *in vivo* in rats or in human, produced a significant accumulation of fatty microvesicles in rat hepatocytes *in vitro*. Hence, this steatotic-like *in vitro* effect of CsA can be considered as an artifact, which has no *in vivo* relevance. RGZ has been shown to be cytotoxic *in vitro* to hepatocytes from different donors ($EC_{(50)} < 100$ μM) (Lloyd et al., 2002). In the present study RGZ was significantly cytotoxic at 50 μM concentration and above. Several studies illustrated a reduction in hepatic steatosis by RGZ in human type 2 diabetic patients (Carey et al., 2002; Mayerson et al., 2002). Here an accumulation of lipid droplets was detected, even though the effect was observed only at late stages of treatment and was associated with cytotoxic effect. These results suggest that the lipid metabolism may be affected following RGZ treatment *in vitro*, but it cannot be excluded that impairment of lipid metabolism represents a secondary effect due to cytotoxicity. The mechanisms leading to hepatocellular injury caused by RGZ are not very well understood. It is possible that the chronic exposure to RGZ, as shown in other studies (Feinstein et al., 2005), could directly interfere with mitochondrial functions, resulting in impairment of mitochondrial β-oxidation of fatty acids leading to steatosis. Likewise, VPA is known to induce cases of steatosis in patients and in some animal models through the inhibition of β-oxidation and the synthesis of fatty acids (Fromenty and Pessayre, 1995; Lee et al., 2007). Abnormal lipid metabolism was observed after acute high dose exposure *in vivo* (Lee et al., 2007) and *in vitro* using HCI approach (Fujimura et al., 2009). In this study conditions, accumulation of lipid following 14 days exposure was not observed. Given the fact that the selected dose range (25–100 μM) was much lower than acute 24-h studies (1–3 mM) (Lee et al., 2008) and C_{max} values found in rat plasma (Blotnik et al., 1996; Ohshiro et al., 2003), it may be speculated that higher concentrations might have been necessary to elicit a steatogenic response. Further incubation of rat hepatocytes with higher concentration of VPA (500–3000 μM) for 72 h resulted into dose-dependent accumulation of neutral lipids (Suppl. Fig. 7).

MET, FFB, IBU and ACT, have not been reported to cause hyperbilirubinemia, steatosis or phospholipidosis after *in vivo* treatment (Table 2), thus served as negative controls for the three specific HCI readouts investigated in our long-term *in vitro* system. Additionally, each of the other selected compounds is a known hepatotoxicant for one specific pathological feature, either for hyperbilirubinemia or steatosis or phospholipidosis. Hence, each compound served as a negative control for the two other studied untoward events, e.g., AMD was considered a positive control for phospholipidosis, but a negative one for hyperbilirubinemia and steatosis. Short-term acute high-concentration *in vitro* toxicity testing of hepatocytes normally turned out to have little predictivity of the hepatotoxicity observed *in vivo*, either in animals or in man (McKim, 2010; Xu et al., 2004). Since the occurrence of hepatotoxicity is a complex process, the use of a panel of tests covering different types of liver injury has been suggested (Guguen-Guillouzo and Guillouzo, 2010). By selecting multiple parameters associated with specific *in vivo* hepatotoxic functions and endpoints, this work represents a more germane approach. Multi-parametric cellular imaging-based approaches have already been used to investigate DILI (Donato et al., 2012; van de Water et al., 2011; Xu et al., 2004, 2008). In these studies, cells have been exposed to compounds up to a maximum of 72 h. In many cases, cell lines without drug metabolizing activity or liver-specific functions were used. For these reasons, they may be regarded as descriptors of acute general organ toxicity rather than specific hepatotoxicity. In general the high concentrations used are significantly exceeding the exposure detected in animals or man, inducing unspecific cytotoxicity confounding interpretations of more liver-specific event. In fact, hepatocytes treated with AMD for 48 h displayed dose-dependent accumulation of phospholipids, but the treatment with high concentrations (10–30 μM) was associated with cytotoxicity (Suppl. Fig. 2). For that purpose subcytotoxic concentrations were always used, which limited the occurrence of unspecific effects. Table 2 shows that the concentrations used for the 2-week hepatocyte treatments were comparable to C_{max} achieved in animal studies and were in the therapeutic exposure range found in patients. In addition, Table 2 summarizes the results obtained under these experimental conditions compared to preclinical and clinical findings. In order to have a more precise *in vitro–in vivo* extrapolation, the use of toxicokinetics data as well as physiologically based toxicokinetics modeling (PBTK) is recommended (Coecke et al., 2013). The nominal concentrations applied to the culture systems may deviate from the actual concentration of the compound due to the occurrence of multiple possible events, such as accumulation, evaporation, binding to plastic and/or medium components, uptake and metabolism (Blaauboer, 2010; Tanneberger et al., 2010). The combination of toxicodynamic and toxicokinetic approaches has been extensively investigated in the EU funded 7th Framework Project Predict-IV. Results obtained support the usefulness of *in vitro* biokinetic data in the interpretation of *in vitro* repeated exposure toxicity data (Broeders et al., 2013; Coecke et al., 2013; Parmentier et al., 2013). Overall, despite the limited number of molecules tested, this approach displayed some sensitivity (able to detect true positives) and specificity (able to detect true negatives) for the prediction of PLD and inhibition of Mrp2-mediated transport. Indeed, on one hand, the treatment of hepatocytes with PLD-inducing compounds (AMD and CPZ) and hyperbilirubinemia/cholestasis-inducing compounds (CsA, TGZ, CPZ) effectively resulted in the expected effects. On the other hand, the predictive value (sensitivity + specificity) for steatosis remained unsatisfactory as the occurrence of false negative and false positive outcome was observed upon treatment with VPA and CsA respectively.

In summary, these results provided evidence that cellular responses to hepatotoxicants can be monitored using high content microscopy. Primary rat hepatocytes cultured in Collagen I/Matrigel™ sandwich configuration have been evaluated and shown to be a suitable system for the investigation of some chronic-like drug-induced toxicity, given the capability to obtain full polarization. By using subtoxic concentrations, this model can indeed mimic the repeated exposure of cells to hepatotoxicants and could be used to improve the prediction of some hepatotoxicity in preclinical development. The analysis aimed at finding parameters that predict toxicity-related events before actual cell death occurred. The data obtained suggested that liver specific functional impairments investigated with cellular imaging technology were enhanced over time and occurred before cytotoxicity.

The limited compound set used in this study allowed the *in vitro* monitoring of PLD induction and Mrp2 inhibition, known to occur in both preclinical species and human. However, a similar approach using human primary hepatocytes could be used to assess more human-specific drug related events. The present work provides an improved *in vitro* chronic-like approach for the safety profiling of future compounds, in order to avoid hepatotoxic molecules.

Conflict of Interest

The authors declare that there are no conflicts of interest.

Transparency Document

The Transparency document associated with this article can be found in the online version.

Acknowledgements

This work was supported by the European Commission 7th Framework Project Predict-IV 202222.

The authors thank Virginie Riebel, Audrey Dietz, Barbara Bertschi, Marianne Schwald, and Elodie Meyer for excellent technical assistance; Kamal Kumar Balavenkatraman, Olivier Grenet, Philippe Couttet and Elaine Tritto for important intellectual contribution.

Appendix A. Supplementary material

Supplementary data associated with this article can be found, in the online version, at http://dx.doi.org/10.1016/j.tiv.2014.05.009.

References

Ballantyne, C.M., Podet, E.J., Patsch, W.P., Harati, Y., Appel, V., Gotto Jr., A.M., Young, J.B., 1989. Effects of cyclosporine therapy on plasma lipoprotein levels. JAMA 262, 53–56.

Barth, A., Bergmann, R., Zaumseil, J., Klinger, W., 1978. Influence of drugs on bile acid excretion. Arch. Toxicol. Suppl., 359–361.

Begriche, K., Massart, J., Robin, M.A., Borgne-Sanchez, A., Fromenty, B., 2011. Drug-induced toxicity on mitochondria and lipid metabolism: mechanistic diversity and deleterious consequences for the liver. J. Hepatol. 54, 773–794.

Berridge, B.R., Chatman, L.A., Odin, M., Schultze, A.E., Losco, P.E., Meehan, J.T., Peters, T., Vonderfecht, S.L., 2007. Phospholipidosis in nonclinical toxicity studies. Toxicol. Pathol. 35, 325.

Blaauboer, B.J., 2010. Biokinetic modeling and in vitro–in vivo extrapolations. J. Toxicol. Environ. Health, Part B 13, 242–252.

Blotnik, S., Bergman, F., Bialer, M., 1996. Disposition of valpromide, valproic acid, and valnoctamide in the brain, liver, plasma, and urine of rats. Drug Metab. Dispos. 24, 560–564.

Bohme, M., Buchler, M., Muller, M., Keppler, D., 1993. Differential inhibition by cyclosporins of primary-active ATP-dependent transporters in the hepatocyte canalicular membrane. FEBS Lett. 333, 193–196.

Bolesta, S., Haber, S.L., 2002. Hepatotoxicity associated with chronic acetaminophen administration in patients without risk factors. Ann. Pharmacother. 36, 331–333.

Borst, P., Zelcer, N., van de Wetering, K., 2006. MRP2 and 3 in health and disease. Cancer Lett. 234, 51–61.

Broeders, J.J., Blaauboer, B.J., Hermens, J.L., 2013. In vitro biokinetics of chlorpromazine and the influence of different dose metrics on effect concentrations for cytotoxicity in Balb/c 3T3, Caco-2 and HepaRG cell cultures. Toxicol. In Vitro 27, 1057–1064.

Carey, D.G., Cowin, G.J., Galloway, G.J., Jones, N.P., Richards, J.C., Biswas, N., Doddrell, D.M., 2002. Effect of rosiglitazone on insulin sensitivity and body composition in type 2 diabetic patients [corrected]. Obes. Res. 10, 1008–1015.

Choi, Y.H., Lee, U., Lee, B.K., Lee, M.G., 2010. Pharmacokinetic interaction between itraconazole and metformin in rats: competitive inhibition of metabolism of each drug by each other via hepatic and intestinal CYP3A1/2. Br. J. Pharmacol. 161, 815–829.

Coecke, S., Pelkonen, O., Leite, S.B., Bernauer, U., Bessems, J.G., Bois, F.Y., Gundert-Remy, U., Loizou, G., Testai, E., Zaldivar, J.M., 2013. Toxicokinetics as a key to the integrated toxicity risk assessment based primarily on non-animal approaches. Toxicol. In Vitro 27, 1570–1577.

Donato, M.T., Tolosa, L., Jimenez, N., Castell, J.V., Gomez-Lechon, M.J., 2012. High-content imaging technology for the evaluation of drug-induced steatosis using a multiparametric cell-based assay. J. Biomol. Screen. 17, 394–400.

Dunn, J.C., Tompkins, R.G., Yarmush, M.L., 1991. Long-term in vitro function of adult hepatocytes in a collagen sandwich configuration. Biotechnol. Prog. 7, 237–245.

Ertorer, M.E., Paydas, S., Sagliker, Y., 1997. Hyperbilirubinemia in a renal transplant patient due to cyclosporin A therapy. Nephron 76, 368.

Farkas, D., Tannenbaum, S.R., 2005. Characterization of chemically induced hepatotoxicity in collagen sandwiches of rat hepatocytes. Toxicol. Sci. 85, 927–934.

Feinstein, D.L., Spagnolo, A., Akar, C., Weinberg, G., Murphy, P., Gavrilyuk, V., Dello, R.C., 2005. Receptor-independent actions of PPAR thiazolidinedione agonists: is mitochondrial function the key? Biochem. Pharmacol. 70, 177–188.

Finsterer, J., Zarrouk, M.S., 2012. Mitochondrial toxicity of antiepileptic drugs and their tolerability in mitochondrial disorders. Expert. Opin. Drug Metab Toxicol. 8, 71–79.

Floyd, J.S., Barbehenn, E., Lurie, P., Wolfe, S.M., 2009. Case series of liver failure associated with rosiglitazone and pioglitazone. Pharmacoepidemiol. Drug Saf 18, 1238–1243.

Foster, J.R., Jacobsen, M., Kenna, G., Schulz-Utermoehl, T., Morikawa, Y., Salmu, J., Wilson, I.D., 2012. Differential effect of troglitazone on the human bile acid transporters, MRP2 and BSEP, in the PXB hepatic chimeric mouse. Toxicol. Pathol. 40, 1106–1116.

Fromenty, B., Pessayre, D., 1995. Inhibition of mitochondrial beta-oxidation as a mechanism of hepatotoxicity. Pharmacol. Ther. 67, 101–154.

Fruncillo, R.J., Bernhard, R., Swanson, B.N., Vlasses, P.H., Ferguson, R.K., 1985. Effect of phenobarbitone on the pharmacokinetics and tissue levels of amiodarone in the rat. J. Pharm. Pharmacol. 37, 729–731.

Fujimura, H., Dekura, E., Kurabe, M., Shimazu, N., Koitabashi, M., Toriumi, W., 2007. Cell-based fluorescence assay for evaluation of new-drugs potential for phospholipidosis in an early stage of drug development. Exp. Toxicol. Pathol. 58, 375–382.

Fujimura, H., Murakami, N., Kurabe, M., Toriumi, W., 2009. In vitro assay for drug-induced hepatosteatosis using rat primary hepatocytes, a fluorescent lipid analog and gene expression analysis. J. Appl. Toxicol. 29, 356–363.

Funk, C., Ponelle, C., Scheuermann, G., Pantze, M., 2001. Cholestatic potential of troglitazone as a possible factor contributing to troglitazone-induced hepatotoxicity: in vivo and in vitro interaction at the canalicular bile salt export pump (Bsep) in the rat. Mol. Pharmacol. 59, 627–635.

Gardner, C.R., Heck, D.E., Yang, C.S., Thomas, P.E., Zhang, X.J., DeGeorge, G.L., Laskin, J.D., Laskin, D.L., 1998. Role of nitric oxide in acetaminophen-induced hepatotoxicity in the rat. Hepatology 27, 748–754.

Gerk, P.M., Vore, M., 2002. Regulation of expression of the multidrug resistance-associated protein 2 (MRP2) and its role in drug disposition. J. Pharmacol. Exp. Ther. 302, 407–415.

Guan, P., Lu, Y., Qi, J., Niu, M., Lian, R., Hu, F., Wu, W., 2011. Enhanced oral bioavailability of cyclosporine A by liposomes containing a bile salt. Int. J. Nanomedicine 6, 965–974.

Guguen-Guillouzo, C., Guillouzo, A., 2010. General review on in vitro hepatocyte models and their applications. Methods Mol. Biol. 640, 1–40.

Halliwell, W.H., 1997. Cationic amphiphilic drug-induced phospholipidosis. Toxicol. Pathol. 25, 53–60.

Hirode, M., Ono, A., Miyagishima, T., Nagao, T., Ohno, Y., Urushidani, T., 2008. Gene expression profiling in rat liver treated with compounds inducing phospholipidosis. Toxicol. Appl. Pharmacol. 229, 290–299.

Hruban, Z., 1984. Pulmonary and generalized lysosomal storage induced by amphiphilic drugs. Environ. Health Perspect. 55, 53–76.

Imamura, Y., Harada, S., Okano, Y., Miyata, T., Otagiri, M., 1988. The effect of metoclopramide on the absorption and pharmacology of chlorpromazine in the rat. J. Pharm. Pharmacol. 40, 116–119.

Ishizaki, J., Ito, S., Jin, M., Shimada, T., Ishigaki, T., Harasawa, Y., Yokogawa, K., Takami, A., Nakao, S., Miyamoto, K., 2008. Mechanism of decrease of oral bioavailability of cyclosporin A during immunotherapy upon coadministration of amphotericin B. Biopharm. Drug Dispos. 29, 195–203.

Kahan, B.D., 1989. Cyclosporine. N. Engl. J. Med. 321, 1725–1738.

Kartenbeck, J., Leuschner, U., Mayer, R., Keppler, D., 1996. Absence of the canalicular isoform of the MRP gene-encoded conjugate export pump from the hepatocytes in Dubin–Johnson syndrome. Hepatology 23, 1061–1066.

Khan, M.S., Akhter, M., 2005. Synthesis, pharmacological activity and hydrolytic behavior of glyceride prodrugs of ibuprofen. Eur. J. Med. Chem. 40, 371–376.

Kim, Y., Lasher, C.D., Milford, L.M., Murali, T.M., Rajagopalan, P., 2010. A comparative study of genome-wide transcriptional profiles of primary hepatocytes in collagen sandwich and monolayer cultures. Tissue Eng. Part C Methods 16, 1449–1460.

Kobayashi, M., Saitoh, H., Kobayashi, M., Tadano, K., Takahashi, Y., Hirano, T., 2004. Cyclosporin A, but not tacrolimus, inhibits the biliary excretion of mycophenolic acid glucuronide possibly mediated by multidrug resistance-associated protein 2 in rats. J. Pharmacol. Exp. Ther. 309, 1029–1035.

Kola, I., Landis, J., 2004. Can the pharmaceutical industry reduce attrition rates? Nat. Rev. Drug Discov. 3, 711–715.

Kuroda, Y., Saito, M., 2010. Prediction of phospholipidosis-inducing potential of drugs by in vitro biochemical and physicochemical assays followed by multivariate analysis. Toxicol. In Vitro 24, 661–668.

Labbe, G., Pessayre, D., Fromenty, B., 2008. Drug-induced liver injury through mitochondrial dysfunction: mechanisms and detection during preclinical safety studies. Fundam. Clin. Pharmacol. 22, 335–353.

Lakshmi, K.S., Rajesh, T., 2011. Rosiglitazone quantification in rat plasma using high performance liquid chromatography with mass spectrometric detection and its application to pre-clinical pharmacokinetic studies. PDA. J. Pharm. Sci. Technol. 65, 100–108.

LeCluyse, E.L., Audus, K.L., Hochman, J.H., 1994. Formation of extensive canalicular networks by rat hepatocytes cultured in collagen-sandwich configuration. Am. J. Physiol. 266, C1764–C1774.

Lal, J., Jain, G.K., 2010. Effect of centchroman coadministration on the pharmacokinetics of metformin in rats. Indian J. Pharmacol. 42, 146–149.

Lee, M.H., Hong, I., Kim, M., Lee, B.H., Kim, J.H., Kang, K.S., Kim, H.L., Yoon, B.I., Chung, H., Kong, G., et al., 2007. Gene expression profiles of murine fatty liver induced by the administration of valproic acid. Toxicol. Appl. Pharmacol. 220, 45–59.

Lee, M.H., Kim, M., Lee, B.H., Kim, J.H., Kang, K.S., Kim, H.L., Yoon, B.I., Chung, H., Kong, G., Lee, M.O., 2008. Subchronic effects of valproic acid on gene expression profiles for lipid metabolism in mouse liver. Toxicol. Appl. Pharmacol. 226, 271–284.

Lewis, J.H., Mullick, F., Ishak, K.G., Ranard, R.C., Ragsdale, B., Perse, R.M., Rusnock, E.J., Wolke, A., Benjamin, S.B., Seeff, L.B., et al., 1990. Histopathologic analysis of suspected amiodarone hepatotoxicity. Hum. Pathol. 21, 59–67.

Lewis, J.H., Zimmerman, H.J., Garrett, C.T., Rosenberg, E., 1982. Valproate-induced hepatic steatogenesis in rats. Hepatology 2, 870–873.

Li, X., Gu, L., Xu, Y., Wang, Y., 2009. Preparation of fenofibrate nanosuspension and study of its pharmacokinetic behavior in rats. Drug Dev. Ind. Pharm. 35, 827–833.

Lloyd, S., Hayden, M.J., Sakai, Y., Fackett, A., Silber, P.M., Hewitt, N.J., Li, A.P., 2002. Differential in vitro hepatotoxicity of troglitazone and rosiglitazone among cryopreserved human hepatocytes from 37 donors. Chem. Biol. Interact. 142, 57–71.

Loi, C.M., Alvey, C.W., Vassos, A.B., Randinitis, E.J., Sedman, A.J., Koup, J.R., 1999. Steady-state pharmacokinetics and dose proportionality of troglitazone and its metabolites. J. Clin. Pharmacol. 39, 920–926.

Mayerson, A.B., Hundal, R.S., Dufour, S., Lebon, V., Befroy, D., Cline, G.W., Enocksson, S., Inzucchi, S.E., Shulman, G.I., Petersen, K.F., 2002. The effects of rosiglitazone on insulin sensitivity, lipolysis, and hepatic and skeletal muscle triglyceride content in patients with type 2 diabetes. Diabetes 51, 797–802.

McDonough, P.M., Agustin, R.M., Ingermanson, R.S., Loy, P.A., Buehrer, B.M., Nicoll, J.B., Prigozhina, N.L., Mikic, I., Price, J.H., 2009. Quantification of lipid droplets and associated proteins in cellular models of obesity via high-content/high-throughput microscopy and automated image analysis. Assay. Drug Dev. Technol. 7, 440–460.

McKim Jr., J.M., 2010. Building a tiered approach to in vitro predictive toxicity screening: a focus on assays with in vivo relevance. Comb. Chem. High Throughput Screen. 13, 188–206.

Menon, K.V.N., Angulo, P., Lindor, K.D., 2001. Severe cholestatic hepatitis from troglitazone in a patient with nonalcoholic steatohepatitis and diabetes mellitus. Am. J. Gastroenterol. 96, 1631–1634.

Morelli, J.K., Buehrle, M., Pognan, F., Barone, L.R., Fieles, W., Ciaccio, P.J., 2006. Validation of an in vitro screen for phospholipidosis using a high-content biology platform. Cell Biol. Toxicol. 22, 15–27.

Myara, A., Cadranel, J.F., Dorent, R., Lunel, F., Bouvier, E., Gerhardt, M., Bernard, B., Ghoussoub, J.J., Cabrol, A., Gandjbakhch, I., et al., 1996. Cyclosporin A-mediated cholestasis in patients with chronic hepatitis after heart transplantation. Eur. J. Gastroenterol. Hepatol. 8, 267–271.

Newa, M., Bhandari, K.H., Kim, J.A., Yoo, B.K., Choi, H.G., Yong, C.S., Woo, J.S., Lyoo, W.S., 2008. Preparation and evaluation of fast dissolving ibuprofen-polyethylene glycol 6000 solid dispersions. Drug Deliv. 15, 355–364.

Obata, T., 1983. Intrahepatic cholestasis and hyperbilirubinemia in ethynyl estradiol and chlorpromazine-treated rats. Gastroenterol. Jpn. 18, 538–548.

Ohshiro, S., Hobara, N., Sakai, M., Hokama, N., Kameya, H., Sakanashi, M., 2003. Effects of salicylate on the pharmacokinetics of valproic acid after oral administration of sodium valproate in rats. Biog. Amines 17, 401–407.

Oikawa, H., Maesawa, C., Sato, R., Oikawa, K., Yamada, H., Oriso, S., Ono, S., Yashima-Abo, A., Kotani, K., Suzuki, K., et al., 2005. Liver cirrhosis induced by long-term administration of a daily low dose of amiodarone: a case report. World J. Gastroenterol. 11, 5394–5397.

Paine, A.J., 1990. The maintenance of cytochrome P-450 in rat hepatocyte culture: some applications of liver cell cultures to the study of drug metabolism, toxicity and the induction of the P-450 system. Chem. Biol. Interact. 74, 1–31.

Paine, A.J., Williams, L.J., Legg, R.F., 1979. Apparent maintenance of cytochrome P 450 by nicotinamide in primary cultures of rat hepatocytes. Life Sci. 24, 2185–2191.

Parmentier, C., Truisi, G.L., Moenks, K., Stanzel, S., Lukas, A., Kopp-Schneider, A., Alexandre, E., Hewitt, P.G., Mueller, S.O., Richert, L., 2013. Transcriptomic hepatotoxicity signature of chlorpromazine after short- and long-term exposure in primary human sandwich cultures. Drug Metab. Dispos. 41, 1835–1842.

Paulusma, C.C., Bosma, P.J., Zaman, G.J., Bakker, C.T., Otter, M., Scheffer, G.L., Scheper, R.J., Borst, P., Oude Elferink, R.P., 1996. Congenital jaundice in rats with a mutation in a multidrug resistance-associated protein gene. Science 271, 1126–1128.

Pedersen, J.M., Matsson, P., Bergstrom, C.A., Norinder, U., Hoogstraate, J., Artursson, P., 2008. Prediction and identification of drug interactions with the human ATP-binding cassette transporter multidrug-resistance associated protein 2 (MRP2; ABCC2). J. Med. Chem. 51, 3275–3287.

Poucell, S., Ireton, J., Valencia-Mayoral, P., Downar, E., Larratt, L., Patterson, J., Blendis, L., Phillips, M.J., 1984. Amiodarone-associated phospholipidosis and fibrosis of the liver Light, immunohistochemical, and electron microscopic studies. Gastroenterology 86, 926–936.

Reasor, M.J., Kacew, S., 2001. Drug-induced phospholipidosis: are there functional consequences? Exp. Biol. Med. (Maywood) 226, 825–830.

Regal, R.E., Billi, J.E., Glazer, H.M., 1987. Phenothiazine-induced cholestatic jaundice. Clin. Pharm. 6, 787–794.

Rodrigues, M., Alves, G., Abrantes, J., Falcao, A., 2012. Herb-drug interaction of Fucus vesiculosus extract and amiodarone in rats: A potential risk for reduced bioavailability of amiodarone in clinical practice. Food Chem. Toxicol. 52C, 121–128.

Roman, I.D., Monte, M.J., Gonzalez-Buitrago, J.M., Esteller, A., Jimenez, R., 1990. Inhibition of hepatocytary vesicular transport by cyclosporin A in the rat: relationship with cholestasis and hyperbilirubinemia. Hepatology 12, 83–91.

Samuels, A.M., Carey, M.C., 1978. Effects of chlorpromazine hydrochloride and its metabolites on Mg^{2+}- and Na^{+}, K^{+}-ATPase activities of canalicular-enriched rat liver plasma membranes. Gastroenterology 74, 1183–1190.

Schurdak, M.E., Vernetti, L.A., Abel, S.J., Thiffault, C., 2007. Adaptation of an in vitro phospholipidosis assay to an automated image analysis system. Toxicol. Mech. Methods 17, 77–86.

Seglen, P.O., 1976. Preparation of isolated rat liver cells. Methods Cell Biol. 13, 29–83.

Shaikh, N.A., Downar, E., Butany, J., 1987. Amiodarone – an inhibitor of phospholipase activity: a comparative study of the inhibitory effects of amiodarone, chloroquine and chlorpromazine. Mol. Cell Biochem. 76, 163–172.

Stone, B.G., Udani, M., Sanghvi, A., Warty, V., Plocki, K., Bedetti, C.D., Van Thiel, D.H., 1987. Cyclosporin A-induced cholestasis. The mechanism in a rat model. Gastroenterology 93, 344–351.

Tang, W., 2007. Drug metabolite profiling and elucidation of drug-induced hepatotoxicity. Expert Opin. Drug Metab. Toxicol. 3, 407–420.

Tanneberger, K., Rico-Rico, A., Kramer, N.I., Busser, F.J., Hermens, J.L., Schirmer, K., 2010. Effects of solvents and dosing procedure on chemical toxicity in cell-based in vitro assays. Environ. Sci. Technol. 44, 4775–4781.

Terui, K., Saito, T., Hishiki, T., Sato, Y., Mitsunaga, T., Yoshida, H., 2011. Hepatic expression of multidrug resistance protein 2 in biliary atresia. Comp. Hepatol. 10, 6.

Tolosa, L., Pinto, S., Donato, M.T., Lahoz, A., Castell, J.V., O'Connor, J.E., Gomez-Lechon, M.J., 2012. Development of a multiparametric cell-based protocol to screen and classify the hepatotoxicity potential of drugs. Toxicol. Sci. 127, 187–198.

Tong, V., Teng, X.W., Chang, T.K., Abbott, F.S., 2005. Valproic acid II: effects on oxidative stress, mitochondrial membrane potential, and cytotoxicity in glutathione-depleted rat hepatocytes. Toxicol. Sci. 86, 436–443.

Tuschl, G., Hrach, J., Walter, Y., Hewitt, P.G., Mueller, S.O., 2009. Serum-free collagen sandwich cultures of adult rat hepatocytes maintain liver-like properties long term: a valuable model for in vitro toxicity and drug-drug interaction studies. Chem. Biol. Interact. 181, 124–137.

van de Water, F.M., Havinga, J., Ravesloot, W.T., Horbach, G.J., Schoonen, W.G., 2011. High content screening analysis of phospholipidosis: validation of a 96-well assay with CHO-K1 and HepG2 cells for the prediction of in vivo based phospholipidosis. Toxicol. In Vitro 25, 1870–1882.

Varanasi, K.K., Potharaju, S., Rajak, S., Veeraraghavan, S., Mallick, P., Vakkalanka, S.K., 2008. Effect of pentoxifylline on the pharmacokinetics of rosiglitazone in Wistar rats. Methods Find. Exp. Clin. Pharmacol. 30, 537–542.

Wiesner, R.H., Ludwig, J., Lindor, K.D., Jorgensen, R.A., Baldus, W.P., Homburger, H.A., Dickson, E.R., 1990. A controlled trial of cyclosporine in the treatment of primary biliary cirrhosis. N. Engl. J. Med. 322, 1419–1424.

Waitzkin, L., 1962. Prolonged hepatic dysfunction after clinical recovery from chlorpromazine jaundice. Gastroenterology 43, 337–339.

Wilke, R.A., Lin, D.W., Roden, D.M., Watkins, P.B., Flockhart, D., Zineh, I., Giacomini, K.M., Krauss, R.M., 2007. Identifying genetic risk factors for serious adverse drug reactions: current progress and challenges. Nat. Rev. Drug Discov. 6, 904–916.

Wolf, A., Müller, S.-O., Hewitt, P., Pfaller, W., Jennings, P., Testai, E., Bois, F., Prieto, P., Price, A., Lukas, A., Richet, L., Guillouzo, A., Leonard, M., Blaauboer, B., Rostami, A., Reinert, K., Honegger, P., Cechelli, R., Kopp-Schneider, A., Weiss, D., Schröder, O., Huber, C., Dekant, W., 2013. Predict-IV project overview (EU grant 202222)-non animal-based toxicity profiling by integrating toxicodynamics and biokinetics. Toxicology Letters 221S, S7.

Xu, J.J., Diaz, D., O'Brien, P.J., 2004. Applications of cytotoxicity assays and pre-lethal mechanistic assays for assessment of human hepatotoxicity potential. Chem. Biol. Interact. 150, 115–128.

Xu, J.J., Henstock, P.V., Dunn, M.C., Smith, A.R., Chabot, J.R., de, G.D., 2008. Cellular imaging predictions of clinical drug-induced liver injury. Toxicol. Sci. 105, 97–105.

Yamada, T., Arai, T., Nagino, M., Oda, K., Shoda, J., Suzuki, H., Sugiyama, Y., Nimura, Y., 2005. Impaired expression of hepatic multidrug resistance protein 2 is associated with posthepatectomy hyperbilirubinemia in patients with biliary cancer. Langenbecks Arch. Surg. 390, 421–429.

Yamamoto, K., Onishi, H., Ito, A., Machida, Y., 2007. In vitro and in vivo evaluation of medicinal carbon granules and tablet on the adsorption of acetaminophen. Int. J. Pharm. 328, 105–111.

Yamasaki, I., Uotsu, N., Yamaguchi, K., Takayanagi, R., Yamada, Y., 2011. Effects of kale ingestion on pharmacokinetics of acetaminophen in rats. Biomed. Res. 32, 357–362.

Zamek-Gliszczynski, M.J., Xiong, H., Patel, N.J., Turncliff, R.Z., Pollack, G.M., Brouwer, K.L., 2003. Pharmacokinetics of 5 (and 6)-carboxy-2′,7′-dichlorofluorescein and its diacetate promoiety in the liver. J. Pharmacol. Exp. Ther. 304, 801–809.

Zhang, G., Terry Jr., A.V., Bartlett, M.G., 2007. Simultaneous determination of five antipsychotic drugs in rat plasma by high performance liquid chromatography with ultraviolet detection. J. Chromatogr. B Analyt. Technol. Biomed. Life Sci. 856, 20–28.

Ziegler, K., Frimmer, M., 1986. Cyclosporin A and a diaziridine derivative inhibit the hepatocellular uptake of chocolate, phalloidin and rifampicin. Biochim. Biophys. Acta 855, 136–142.

Zimmerman, H.J., Ishak, K.G., 1982. Valproate-induced hepatic injury: analyses of 23 fatal cases. Hepatology 2, 591–597.